








## Human lung-resident mucosal-associated invariant T cells are abundant, express antimicrobial proteins, and are cytokine responsive

Erin W. Meermeier <sup>1,11</sup>, Christina L. Zheng<sup>2</sup>, Jessica G. Tran<sup>3</sup>, Shogo Soma <sup>1</sup>, Aneta H. Worley<sup>3</sup>, David I. Weiss <sup>4</sup>, Robert L. Modlin<sup>5</sup>, Gwendolyn Swarbrick <sup>1,3</sup>, Elham Karamooz<sup>1,3</sup>, Sharon Khuzwayo<sup>6,7</sup>, Emily B. Wong <sup>6,7,8,9,10</sup>, Marielle C. Gold <sup>1,3</sup> & David M. Lewinsohn <sup>1,3</sup>✉

Mucosal-associated Invariant T (MAIT) cells are an innate-like T cell subset that recognize a broad array of microbial pathogens, including respiratory pathogens. Here we investigate the transcriptional profile of MAIT cells localized to the human lung, and postulate that MAIT cells may play a role in maintaining homeostasis at this mucosal barrier. Using the MR1/5-OP-RU tetramer, we identified MAIT cells and non-MAIT CD8<sup>+</sup> T cells in lung tissue not suitable for transplant from human donors. We used RNA-sequencing of MAIT cells compared to non-MAIT CD8<sup>+</sup> T cells to define the transcriptome of MAIT cells in the human lung. We show that, as a population, lung MAIT cells are polycytotoxic, secrete the directly antimicrobial molecule IL-26, express genes associated with persistence, and selectively express cytokine and chemokine-related molecules distinct from other lung-resident CD8<sup>+</sup> T cells, such as interferon- $\gamma$ - and IL-12- receptors. These data highlight MAIT cells' predisposition to rapid pro-inflammatory cytokine responsiveness and antimicrobial mechanisms in human lung tissue, concordant with findings of blood-derived counterparts, and support a function for MAIT cells as early sensors in the defense of respiratory barrier function.

<sup>1</sup>Department of Pulmonary and Critical Care Medicine, Oregon Health & Science University, Portland, OR 97239, USA. <sup>2</sup>Department of Medical Informatics and Clinical Epidemiology, Oregon Health & Science University, Portland, OR 97239, USA. <sup>3</sup>VA Portland Health Care System, Portland, OR 97239, USA. <sup>4</sup>David Geffen School of Medicine at UCLA, Los Angeles, CA 90095, USA. <sup>5</sup>Division of Dermatology, Department of Medicine, David Geffen School of Medicine at University of California, Los Angeles, Los Angeles, CA 90095, USA. <sup>6</sup>Africa Health Research Institute, Durban, South Africa. <sup>7</sup>School of Laboratory Medicine and Medical Sciences, University of KwaZulu-Natal, Durban, South Africa. <sup>8</sup>Division of Infectious Diseases, Massachusetts General Hospital, Boston, MA, USA. <sup>9</sup>Harvard Medical School, Boston, MA, USA. <sup>10</sup>Division of Infection and Immunity, University College London, London, UK. <sup>11</sup>Present address: Department of Medicine, Division of Hematology/Oncology, Mayo Clinic, Scottsdale, AZ 85259, USA. ✉email: [lewinsod@ohsu.edu](mailto:lewinsod@ohsu.edu)

The mucosal surface of the lung constitutes one of the most significant portals of entry for pathogenic microbes. Due to the vital nature of its gas exchange function, cellular immune responses in the respiratory tract need to be poised, efficient, and regulated for appropriate defensive functions. Thus, the organization of a regulatory network of immune cells in the respiratory tract plays an important role in maintaining tissue integrity and defending against microbial invasions. Human mucosal-associated invariant T (MAIT) cells are a unique T cell population found in all humans that are characterized by the use of a semi-invariant T cell receptor (TCR)  $\alpha$ -chain, dependence on the non-classical MHC Class I-related molecule MR1, and their rapid effector function. MAIT cells are a subset of T cells restricted by MR1, and are able to recognize infection by a broad array of pathogens, including respiratory pathogens.

Collectively, *in vivo* models of lung infection link MAIT cells to the early stages of bacterial containment in the respiratory tract and in shaping the ensuing adaptive immune response<sup>1–5</sup>. MAIT cell accumulation and expansion at the site of infection depended upon local antigen in conjunction with costimulation from bacteria or TLR signals. Postnatally, MAIT cells expand rapidly in mice in a manner that depends on translocation of MAIT cell antigens such as 5-(2-oxopropylideneamino)-6-D-ribitylamino-uracil (5-OP-RU)<sup>6,7</sup>. In humans, while MAIT cells are present as effectors in both thymus and cord blood<sup>8,9</sup> the expansion of canonical MAIT cells occurs rapidly, and would be consistent with the hypothesis that expansion of MAIT cells may be associated with the neonatal development of the microbiome. Supporting a role for MAIT cells in human host-defense, an individual, found to have a mutation in *MR1* resulting in the absence of MAIT cells, presented with reoccurring infectious diseases at mucosal surfaces<sup>10</sup>. At present an in-depth analysis into biological pathways and effector functions used by MAIT cells in the human lung has not been performed. Thus, we sought to stringently define functional characteristics of MAIT cells residing in lung tissue.

A striking observation of MAIT cells is their presence at mucosal tissue sites but whether they form a distinct functional T cell subset remains unclear. MAIT cells were first discovered by their abundance in the gut lamina propria of humans and mice<sup>11</sup> and are developmentally predisposed to reside in mucosal sites early in life. In support of this, MAIT cells in the thymus, cord blood and peripheral blood express significantly less CD62L, a selectin associated with homing to lymphoid tissues<sup>8</sup>. Moreover, MAIT cells in human 2nd trimester fetuses already express CD45RO and are functionally mature in mucosal tissues, suggesting the development of an early arm of antibacterial mucosal immunity<sup>12</sup>. A study by Salou et al., used transcriptomics, parabiosis, and thymocyte adoptive transfer in mice to show that MAIT and NKT cell subsets share a common differentiation program which is associated with tissue residence<sup>13</sup>. Here, in contrast to other organs, the authors noted that MAIT cells in the lung had slower rates of parabiotic exchange. The authors suggest that a preset transcriptional program predisposes MAIT cells to reside in tissues. We found that MAIT cells with mycobacterial reactivity are present in the airways of healthy individuals, and further enriched in bronchoalveolar fluid isolated from patients with active pulmonary tuberculosis<sup>14</sup>. Furthermore, bronchoalveolar MAIT cells from healthy individuals with latent tuberculosis produce less pro-inflammatory cytokines, display higher levels of inhibitory markers, and can express distinct tissue repair genes compared to peripheral MAIT cells<sup>15</sup>. Finally, murine models of bacterial pneumonia have uncovered a key role for MAIT cells in the lungs that proliferate *in situ* as opposed to being recruited from lymph nodes<sup>16</sup>. Examination of the function of human lung-derived

MAIT cells has been underexplored, and we do not yet know whether they form a functionally distinct T cell subset compared to other CD8<sup>+</sup> lung-resident T cells.

MAIT cells derived from different tissues have a phenotype and function consistent with their anatomic, microbial, and inflammatory microenvironment. Upon stimulation, MAIT cells produce a variety of cytokines that have the potential to promote an antibacterial or anti-fungal response. It has been widely observed that they produce the pro-inflammatory cytokines IFN- $\gamma$  and TNF but also IL-17 and IL-22 in certain tissues and disease states<sup>12,17–21</sup>. Analysis of human intestinal MAIT cells shows transcripts but not corresponding proteins of proinflammatory cytokines suggesting a degree of post-transcriptional regulation<sup>22</sup>. MAIT cells also express cytotoxic molecules and are capable of lysing target cells ranging from macrophages to epithelial cells<sup>23–25</sup>. The cytotoxic potential of MAIT cells can be licensed by bacterial infection, TCR stimulation, or cytokines including IL-7, IL-12, IL-15, and IL-18<sup>23,25–27</sup>. However, the inflammatory state and cytotoxic potential of MAIT cells in the human lung remains unclear.

Here, we sought to address the hypothesis that MAIT cells in the lung have unique transcriptionally-defined effector functions for their critical role in early recognition and control of respiratory pathogens. We took a comprehensive approach to define the transcriptome of human lung-derived MAIT cells compared to paired non-MAIT CD8<sup>+</sup> T cells. Our analysis reveals MAIT cell's comprehensive repertoire of cytokine and chemokine receptors including the IL-12 receptor and IFN- $\gamma$  receptor, and expression and induction of cytolytic molecules for their antimicrobial capacity, such as IL-26 and granzyme B. Our findings align with the paradigm of MAIT cells as a lung-enriched cell type armed for specialized defense against initial pathogen encounters.

## Results

**MAIT cells are enriched in the lungs.** To identify MAIT cells in the lung parenchyma, we used human lungs not suitable for transplant as an essential source of lung-derived immune cells through a collaboration with the Pacific Northwest Transplant Bank in Portland, Oregon (Supplementary Table 1). Unfortunately, matched peripheral blood was not available from these donors. We used flow cytometry and a MR1-tetramer bound with either an activating ligand, 5-OP-RU (MR1/5-OP-RU), or a non-activating ligand, 6-formyl pterin, 6-FP (MR1/6-FP). We quantified MAIT cells as a proportion of all live CD3<sup>+</sup> T cells that stained with MR1/5-OP-RU above the minimal background staining with MR1/6-FP (Fig. 1a). MAIT cells comprised a higher proportion of all CD3<sup>+</sup> T cells in the lung (median 2.15%, range 0.37–4.90%) compared to those from PBMC (median 0.93%, range 0.27–1.29%) ( $p = 0.004$ ) (Fig. 1b). In contrast to MAIT cells from PBMC, roughly half of the MAIT cells in the lung did not express high levels of the co-receptors CD8 or CD4 (CD8<sup>–</sup>CD4<sup>–</sup>) (median 57%) (Fig. 1a, c). Figure 1a shows two examples of co-receptor expression by MAIT cells. This pattern of CD8 or CD4 expression was also mirrored by non-MAIT lung derived CD3<sup>+</sup> T cells (Fig. 1c). As the proportion of CD8<sup>–</sup>CD4<sup>–</sup> cells was higher than expected, we postulated that this diminished co-receptor expression was the result of the enzymatic processing of the lung tissue. However, we were readily able to discern these populations in the lung by flow cytometry (Supplementary Fig. 1). MAIT cells in the lung, as has been established for MAIT cells in the blood, are of the effector memory T cell compartment (Fig. 1d, e). Similarly, the majority of CD4<sup>–</sup> T cells within matched lung donors were also within the effector memory T cell compartment. On average, as a subset of CD3<sup>+</sup> T cells, MR1-tetramer<sup>+</sup> MAIT cells are 2.3-fold more abundant in the lung than in the

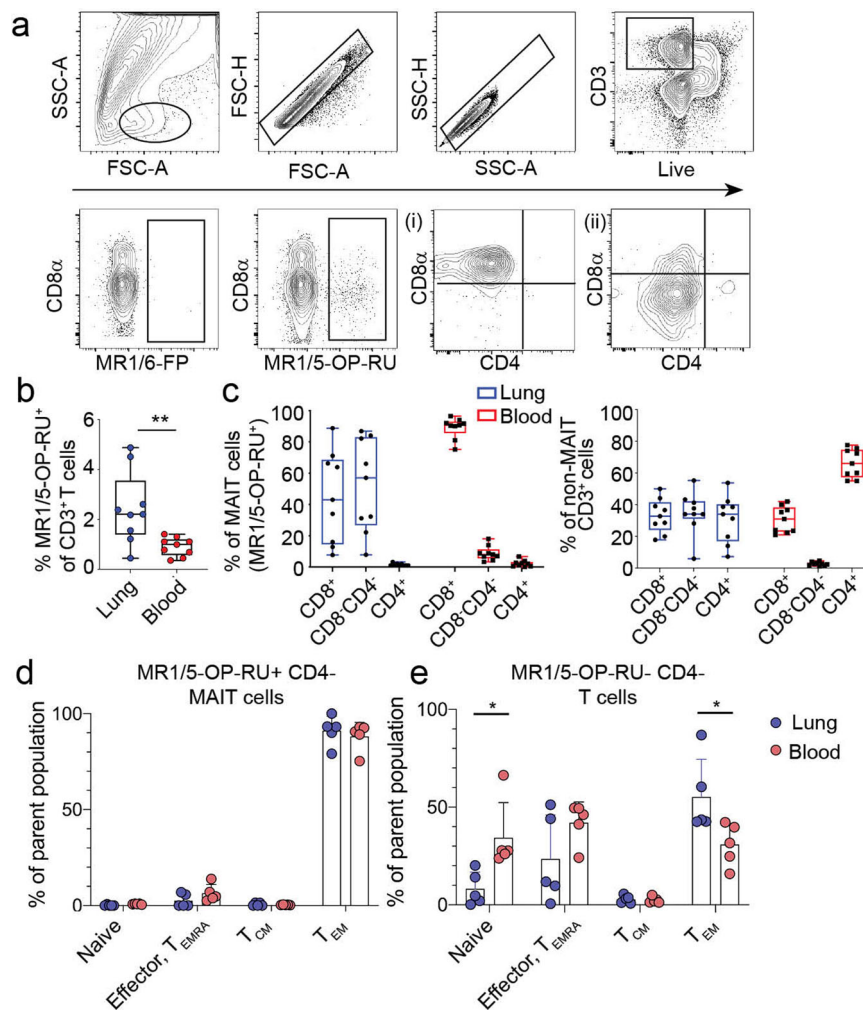


**Fig. 1 MR1-tetramer<sup>+</sup> MAIT cells are an abundant T cell subset in the human lung.** Lung-derived cells were stained with antibodies to T cell identification markers and the MR1-tetramer displaying either the activating 5-OP-RU ligand or the inert 6-FP ligand. **a** MAIT cells were identified by the gating strategy shown on an example lung tissue as CD3<sup>+</sup> MR1/5-OP-RU<sup>+</sup>. Staining with MR1-tetramer/6-FP was used as a negative control. MR1/5-OP-RU<sup>+</sup> cells are plotted by CD4 vs. CD8 $\alpha$  expression where (i) shows a lung sample where the majority of MAIT cells express CD8 $\alpha$  while (ii) shows a sample where MAIT cells were mostly CD8<sup>-</sup>CD4<sup>-</sup>. **b** Frequencies of MR1/5-OP-RU<sup>+</sup> cells of total CD3<sup>+</sup> T cells in lung parenchyma compared to the PBMC are shown by box plot. Horizontal bars indicate the median values. Statistical significance of the difference between groups was determined using the nonparametric Mann-Whitney U-test. \*\*  $P < 0.01$ ,  $n = 9$  per tissue, age range of lung donors 6–64 years. **c** MR1/5-OP-RU<sup>+</sup> MAIT cells (left) or non-MAIT T cells (right) were stained for their expression of CD4 and CD8 co-receptor by flow cytometry. Cells derived from lung samples are summarized by blue box plots, PBMC samples by red box plots,  $n = 9$  per tissue. Graphs showing the % of **(d)** MR1/5-OP-RU<sup>+</sup> CD4<sup>-</sup> MAIT cells or **(e)** MR1/5-OP-RU<sup>-</sup> CD4<sup>-</sup> T cells in the lung and PBMC within common CD8<sup>+</sup> T cell memory compartments. T cells were identified as naïve (CD45RO<sup>-</sup>, CD62L<sup>+</sup>, CCR7<sup>+</sup>), effector or TEMRA (CD45RO<sup>-</sup>, CD45RA<sup>+</sup> or (–) CD62L<sup>-</sup>, CCR7<sup>-</sup>), central memory (CD45RO<sup>+</sup>, CD62L<sup>+</sup>, CCR7<sup>+</sup>), and effector memory (CD45RO<sup>+</sup>, CD62L<sup>-</sup>, CCR7<sup>-</sup>). Age range of lung donors: 22–51 years \* $P < 0.05$ ,  $n = 5$  per tissue, SD shown.

blood, show heterogeneity based on co-receptor expression, and exclusively display an effector memory T cell phenotype.

**RNA-sequencing of human lung-derived MAIT cells.** To determine if MAIT cells from the lung display a profile distinct from non-MAIT CD8<sup>+</sup> T cells, we performed differential gene expression analysis on CD8<sup>+</sup> MAIT cells and CD8<sup>+</sup> non-MAIT cells isolated from the same lung. MAIT cells were identified by staining with the MR1/5-OP-RU tetramer and expression of CD8 (Fig. 2a red gates). Non-MAIT CD8<sup>+</sup> T cells were defined by absence of staining with the MR1/5-OP-RU tetramer and expression of CD8. Matched MAIT and non-MAIT cells were collected from four different donors and RNA-sequencing was performed. While we also collected, and performed gene expression analysis on both the CD8<sup>+</sup> and the CD8<sup>-</sup> CD4<sup>-</sup>, tetramer positive cells, we have focused on the CD8<sup>+</sup> cells as we

did not find major differences in these populations using principal component analysis. Additionally, we found that sorting based on the expression of the co-receptor enhanced the quality of the gene-expression analysis in that we did not observe evidence for B cell contamination that while rare, might have been the result of non-specific tetramer binding. Gene signatures of human lung resident CD8<sup>+</sup> T cells have recently been published<sup>28,29</sup>. We observed that the MAIT and non-MAIT cells derived from lung tissue expressed many tissue residency-associated transcripts, such as CD69 and CD103 (*ITGAE*), supporting that our cells were derived from the lung tissue not vasculature (Supplementary Fig. 2).

**The distinct transcriptome of lung-derived MAIT cells as compared to non-MAIT CD8<sup>+</sup> T cells.** Differential gene expression analysis of the lung samples showed a large number of

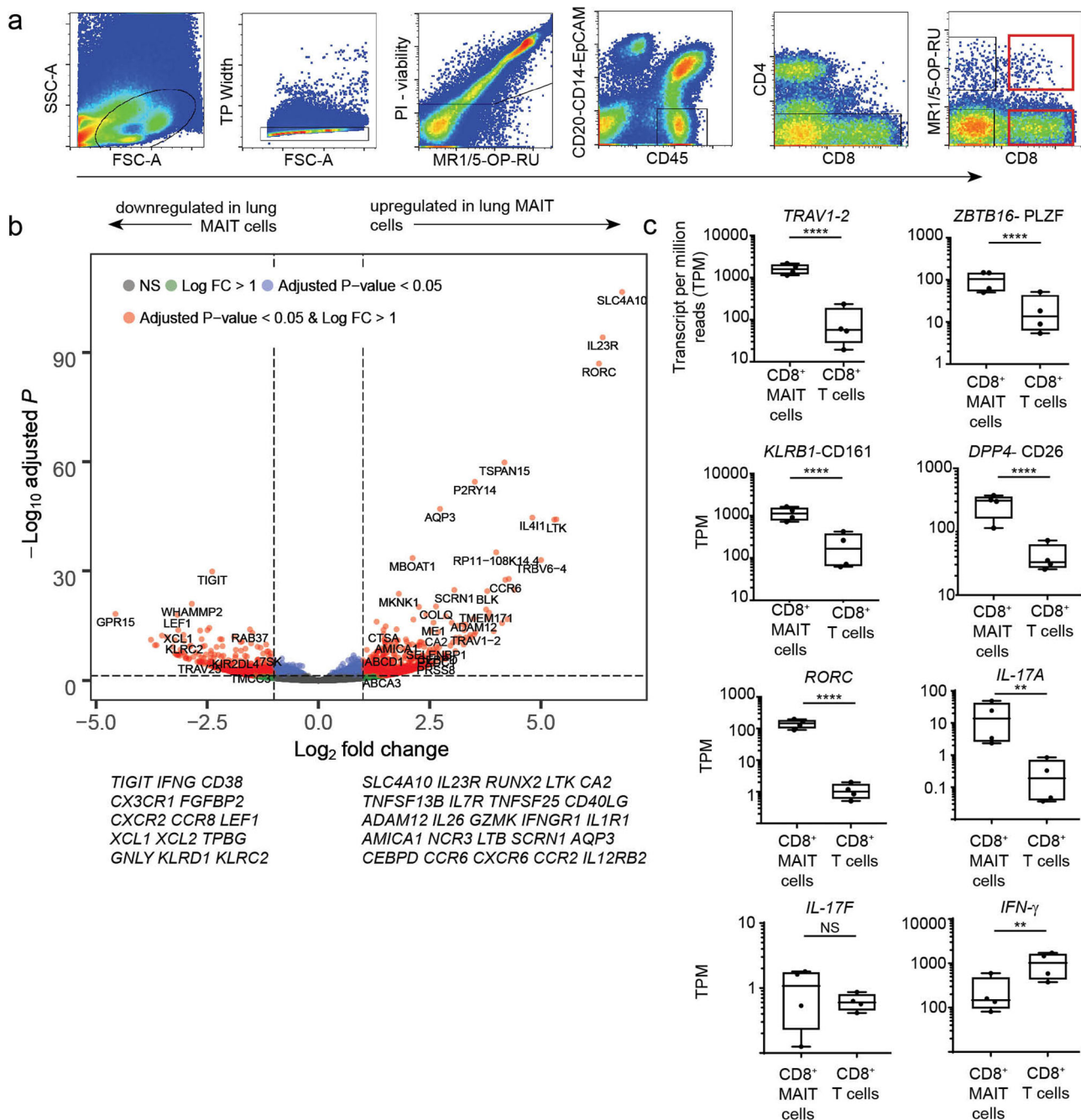


**Fig. 2 RNA-seq profiling of MAIT cell and CD8<sup>+</sup> T cell subsets in human lungs.** RNA-sequencing was performed on T cells from four lung samples and five PBMC samples that were FACS-sorted using the gating strategy shown in (a). Sorted MAIT cells were PI-/CD45+/CD20-CD14-EpCAM-/CD4- and MR1/5-OP-RU+ and CD8<sup>+</sup>. Non-MAIT cells were PI-/CD45+/CD20-CD14-EpCAM-/CD4- and CD8<sup>+</sup>. A representative FACS plot from a lung sample is shown. Age range of lung donors: 11–67 years. **b** Volcano plot depicting differentially expressed genes of lung-derived CD8<sup>+</sup> MAIT cells compared to non-MAIT CD8<sup>+</sup> T cells. Significantly differentially expressed genes (log<sub>2</sub> fold change >1 or <–1, and FDR *P*-value ≤ 0.05) are represented as red. Less significantly different genes are represented as blue, green or gray depending upon the significance thresholds that they fell below. **c** Box plots of transcript per million (TPM) reads of genes commonly associated with MAIT cells, from RNA-seq samples of CD8<sup>+</sup> MAIT cells or non-MAIT CD8<sup>+</sup> T cells derived from four lung samples. Box plots indicate the median and range of the TPM RNA-seq reads. FDR \**P* < 0.05, \*\**P* < 0.01, \*\*\*\**P* < 0.0001.

genes significantly (FDR-adjusted *P*-value ≤ 0.05) expressed in MAIT cells as compared to non-MAIT CD8<sup>+</sup> T cells (Fig. 2b and Supplementary Data 2). Many upregulated genes are in line with transcriptional profiles of MAIT cells in the blood, suggesting an underlying homogenous program in MAIT cell populations, extending to those residing in the human lung<sup>30–33</sup> (Fig. 2b and Supplementary Data 2). Significantly expressed genes identified within MAIT cells in the lung included genes associated with

MAIT cell identity and function, such as the invariant TCR *TRAV1-2*, the transcription factors *ZBTB16* (PLZF) and *RORC*, *DPP4* (CD26), *KLRB1* (CD161) (Fig. 2c) and *IL23R*. In addition to *RORC*, we found robust expression of *IL17A* (Fig. 2c), concordant with our observations in both peripheral blood<sup>34</sup> and the lung<sup>15</sup>. The highest significantly upregulated gene in lung MAIT cells was *SLC4A10*. *SLC4A10* encodes a sodium bicarbonate transporter NCBE, possibly associated with pH homeostasis.



Similarly, we found preferential expression of *CA2*, a gene associated with pH homeostasis, but whose function in T cells is not known. Genes associated with long term survival of T cells including *RUNX2*, which plays a T cell intrinsic role in the long-term persistence of memory  $CD8^+$  T cells after LCMV infection in mice<sup>35</sup>, *LTK*, *TNFSF13B*, *IL7R*, and *TNFSF25* were more highly expressed by MAIT cells. Specific costimulatory receptors were also enriched in MAIT cells including *CD40LG* and *ADAM12*<sup>36</sup>. The MAIT cell population differentially expressed the following cytotoxicity related-genes: *IL26*, *GZMK*, *IL1RI*, *AMICA1*, *NCR3*, *LTB*, and *SCRN1*. Interestingly, MAIT cells in the lung expressed high levels of transcript for cytotoxic molecule granzyme B which contrast with the low granzyme B expression that has been reported in circulating MAIT cells<sup>23</sup>. Finally, genes involved in cell extravasation and recruitment to inflamed tissue including *CEBPD*<sup>37</sup> (CCAAT/enhancer-binding protein delta), *CCR6*, *AQP3*, *CXCR6*, *CCR2*, and *CCR1* were more highly expressed in lung MAIT cells.

We also found genes that were significantly less expressed in the MAIT cell population compared to the non-MAIT lung derived  $CD8^+$  T cells. Some of these genes are associated with T cell activation after antigen experience, and include, *IFNG*, *CD38*, *CX3CR1*, *TIGIT*, *FGFBP2*, *CXCR2*, and *CCR8* (Fig. 2b and Supplementary Data 2). *LEF1*, a transcription factor in the WNT/ $\beta$ -catenin pathway, was also significantly downregulated in lung MAIT cells compared to lung non-MAIT cells. Moreover, an inhibitor of the WNT/ $\beta$ -catenin pathway was more highly expressed in lung MAIT cells, *TPBG*. Lastly, MAIT cells expressed less of the genes encoding the innate receptors *CD94* and *NKG2C* (*KLRD1*, *KLRC2*) than non-MAIT  $CD8^+$  T cells, genes associated with TCR independent activation of MAIT cells in the blood<sup>19</sup>.

Upon pathway analysis of the lung MAIT cell associated genes, we found them to be enriched with the Cytokine-Cytokine receptor interaction (hsa04060) KEGG pathway (Fig. 3a); thus suggesting unique pathways of sensing the lung microenvironment by MAIT cells. As shown in Fig. 3, unsupervised clustering reveals subsets of cytokines, chemokines, and receptors that are significantly differentially expressed within lung MAIT cells compared to non-MAIT  $CD8^+$  T cells. We validated two of these gene patterns with qPCR using an additional cohort of three lung organ donors and the gene *CD3E* as a positive control. For the *IL26* gene, transcript was found in MAIT cells in two of three donors and not in non-MAIT  $CD8^+$  T cells (Fig. 3b). For *CXCR6*, encoding a receptor which can integrate epidermal innate immune chemokine signals, we observed higher transcript in all three additional lung MAIT cell samples (Fig. 3b). These data help to delineate cytokine signaling pathways that MAIT cells could use for environmental surveillance as well as modulation of local inflammation at lung barrier tissue. Collectively, genes differentially expressed by lung MAIT cells are associated with amplifying pro-inflammatory signals and T cell chemotactic ligands.

**$CD8^+$  and  $CD8^-CD4^-$  MAIT cells derived from the lung share a similar transcriptomic profile.** As described above, we have been able to derive a core set of genes associated with lung-resident  $CD8^+$  MAIT cells. As  $CD8^-CD4^-$  MAIT cells are common in the lung (Fig. 1), we wanted to understand whether they shared the same core gene set as  $CD8^+$  MAIT cells. A study by Dias et al. found that blood-derived  $CD8^-CD4^-$  MAIT cells were functionally distinct from MAIT cells expressing  $CD8$ <sup>32</sup> and that  $CD8^-CD4^-$  MAIT cells reflect an activated pool of  $CD8^+$  MAIT cells. Using qPCR, we confirmed that *CD8* gene expression was present uniquely on the  $CD8^+$  subset (Supplementary Fig. 3).

To independently derive a gene set for  $CD8^-CD4^-$  MAIT cells, we analyzed differential gene expression within the transcriptomes of lung  $CD8^-CD4^-$  MAIT and  $CD8^-CD4^-$  non-MAIT cells from four lung donors. Here, we defined genes significantly ( $FDR \leq 0.05$ ) expressed in  $CD8^-CD4^-$  MAIT cells as compared to  $CD8^-CD4^-$  non-MAIT cells (Supplementary Fig. 3). This analysis revealed a highly similar gene expression pattern to the one derived for  $CD8^+$  MAIT cells (Fig. 2b). As we did not observe differences in the activation status, we postulate that these populations reflect similar transient activation histories in the lung. These data also support our earlier comparative emphasis on  $CD8^+$  cells.

### **MAIT cells in the lung have a polycytotoxic phenotype and secrete IL-26.**

Cytolytic properties of immune cells, including MAIT cells, are associated with the elimination of intracellular bacterial infection, either through the induction of apoptosis of the target cells, or via the introduction of anti-bacterial proteins. Traditionally in humans, cytotoxic  $CD8^+$  and  $CD4^+$  T cells contain granzyme B, perforin, and granulysin in preformed granules, allowing for rapid delivery to the target cell<sup>38–41</sup>. MAIT cells also express cytotoxic molecules and are capable of lysing bacterially infected cells ranging from macrophages to epithelial cells. MAIT cell degranulation is associated with MR1 antigen presentation<sup>24</sup>. Circulating MAIT cells express less granzyme B compared to non-MAIT T cells<sup>23</sup>. They must be licensed to produce granzyme B in the context of infection, TCR or MR1-independent cytokine stimulation. Proteomics analysis of blood-derived MAIT cells identified multiple cytotoxicity-related proteins with pronounced expression in MAIT cells, compared to non-MAIT  $CD8^+$  T cells, in the context of *E. coli* infection<sup>42</sup>. Correspondingly lung-derived MAIT cells expressed high levels of transcript for traditional cytolytic proteins including granzyme B, granzyme A, granzyme K, perforin, and granulysin (Fig. 4a, Supplementary Data 2). Cytotoxicity related-genes specifically enriched in MAIT cells over non-MAIT  $CD8^+$  T cells included: *IL26*, *GZMK*, *LTB*, *IL1RI*, *AMICA1*, *NCR3*, and *SCRN1*. Through populational RNA-seq analysis, we could not distinguish whether differences were at the individual cell level or the population level.

Through populational RNA-seq analysis, we could not distinguish whether differences were at the individual cell level or the population level.

To validate the repertoire of preformed cytotoxic proteins in lung MAIT cells compared to non-MAIT cells at the single cell level, we used flow cytometry as well as ELISA of cell supernatants. We used intracellular flow cytometry on ex vivo lung samples to measure expression of proteins corresponding to the genes listed in Fig. 4a at the single cell level. In concordance with the gene expression patterns, a high proportion of lung-derived MAIT cells and  $CD8^+$  non-MAIT cells expressed preformed cytotoxic proteins. We observed a trend of more MAIT cells expressing granzyme A and K compared to non-MAIT  $CD8^+$  lung T cells. Specifically, on average, 62%, 52%, 50%, 63%, and 17% of MAIT cells expressed preformed granzyme B, granzyme A, granzyme K, perforin, and granulysin in the lung, respectively (Fig. 4b). In contrast, 60%, 34%, 30%, 69%, and 18% of non-MAIT  $CD8^+$  T cells in the lung expressed granzyme B, granzyme A, granzyme K, perforin, and granulysin, respectively. A minority of  $CD4^+$  T cells in the lung expressed cytotoxic proteins. To compare the levels of cytotoxic proteins between MAIT cells derived from lung and blood, we next assessed the intracellular levels of the same proteins from T cell populations in PBMC donors (Fig. 4c). While a significantly higher proportion of MAIT cells from the blood express granzyme A, granzyme K, perforin, and granulysin than non-MAIT  $CD8^+$  T cells, they also

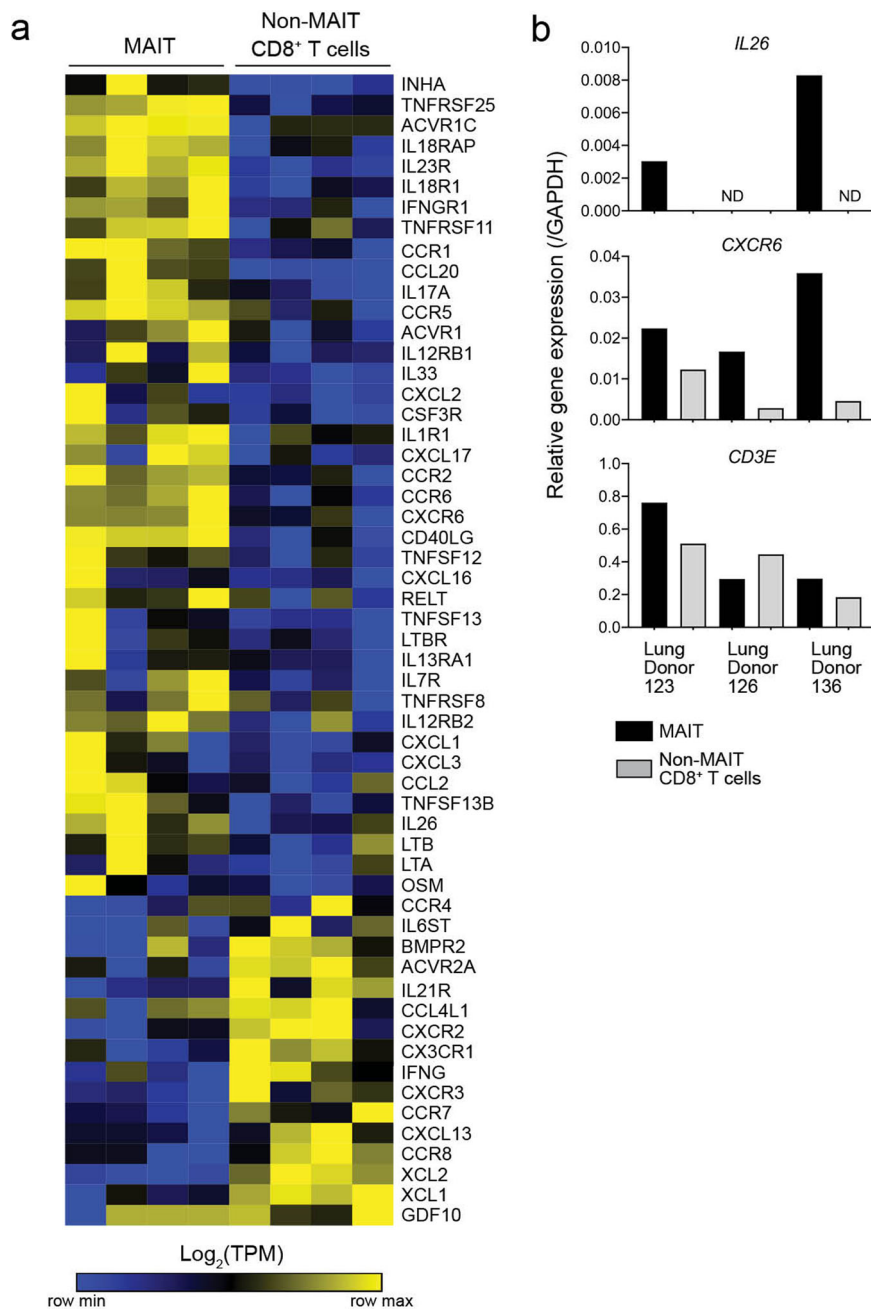


**Fig. 3 Selective expression of cytokine and cytokine receptor genes by MAIT cells in the lung. a** A heatmap showing transcripts per million reads (TPM) of cytokine and cytokine receptor (KEGG: hsa04060) gene expression in CD8<sup>+</sup> MAIT cells and CD8<sup>+</sup> non-MAIT cells (matched) from four lung donors, normalized by row (key). Genes selected from KEGG pathway were differentially expressed by MAIT or non-MAIT CD8<sup>+</sup> T cells (FDR  $\leq$  0.05) and had an average TPM > 10 in at least one of the two subsets of cells. Genes and samples ordered by unsupervised hierarchical clustering using one minus spearman rank correlation. **b** Bar graphs displaying quantitative PCR relative gene expression of *IL26*, *CXCR6*, and *CD3E*, normalized to each sample's expression of *GAPDH*. Samples comprised of MAIT cells or non-MAIT CD8<sup>+</sup> T cells were FACS-sorted from three additional lung donors from those in **a**. Samples were tested in triplicate and averages are displayed. Age range of lung donors: 22–51 years.

expressed less granzyme B than non-MAIT CD8<sup>+</sup> T cells and lung-derived MAIT cells (Fig. 4b versus 4c, granzyme B). Overall, we found more heterogeneity in the frequency of each cell type's expression of cytotoxic proteins in the lung, which could indicate infection history, priming environment, or recent exposure to activating ligand in the lung. Polycytotoxicity has been defined as the co-expression of perforin, granzyme, and granzyme<sup>43</sup>. Therefore, MAIT cells represent a polycytotoxic T cell population in the lung, and in contrast to MAIT cells in the blood, express preformed granzyme B.

Lung-derived MAIT cells expressed significant higher levels of *IL26* (Figs. 3b, 4a). *IL-26* is an *IL-20* family cytokine that signals via a heterodimeric receptor expressed on epithelial cells<sup>44,45</sup>. It has both signaling characteristics and cationic properties that allow it to bind to DNA and also disrupt bacterial membranes<sup>46</sup>. Interesting, *IL-26* has direct antimicrobial activity against mycobacteria, including *Mycobacterium tuberculosis*<sup>47</sup>. Transcriptomic studies of blood derived MAIT cells show presence of *IL26* upon stimulation through the TCR or with *IL-12/18*<sup>48,31,49</sup>. We used ELISA to determine the presence of *IL-26*

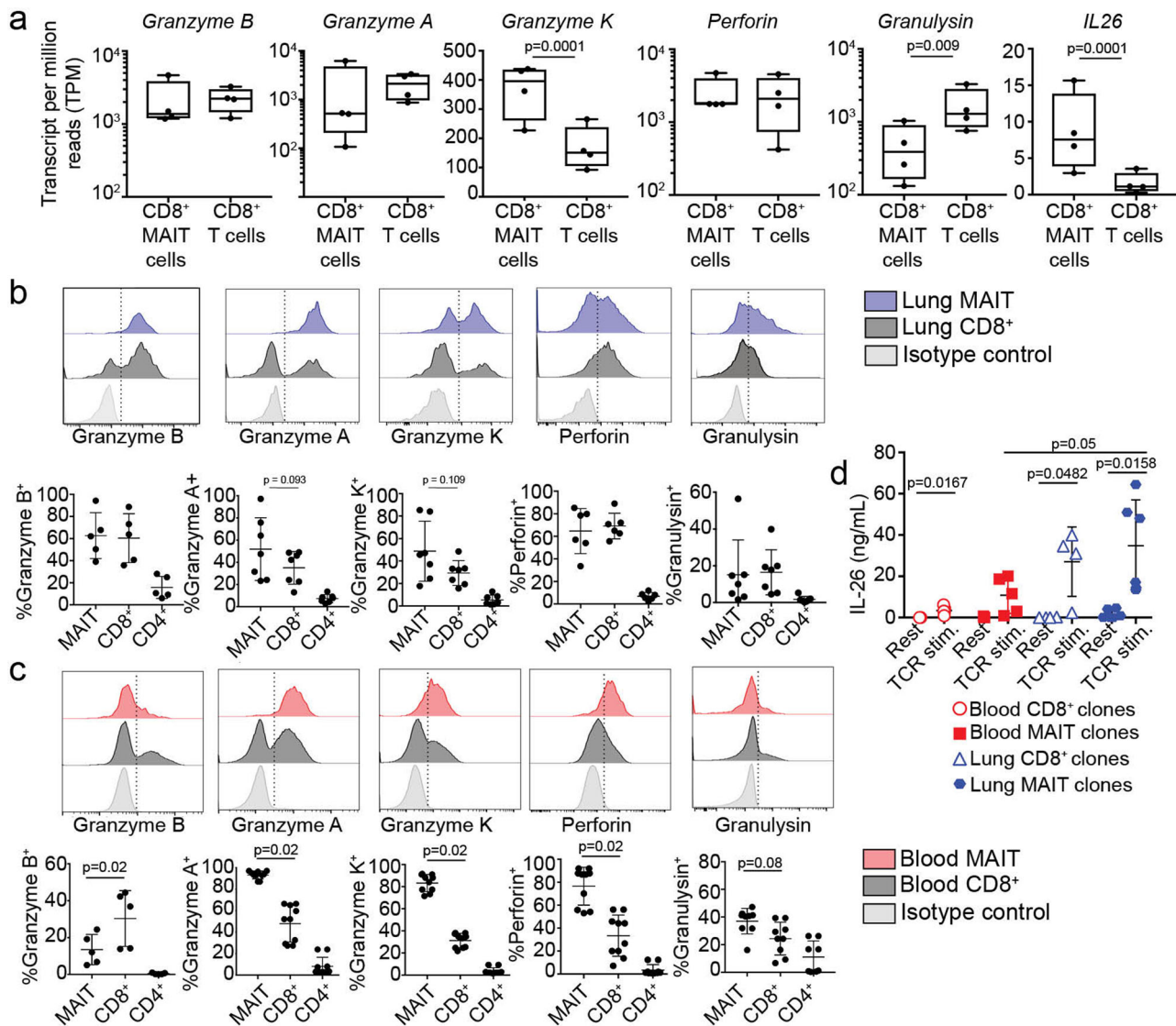


**Fig. 4** MAIT cells in the lung are enriched for preformed cytotoxic molecules and can produce IL-26. **a** Transcripts per million (TPM) reads of cytotoxic T cell function related genes from paired lung RNA-seq samples,  $n = 4$ . **b** Flow cytometry on lung samples to measure intracellular levels of pre-formed cytotoxic molecules in MAIT cells (blue) or non-MAIT CD8<sup>+</sup> T cells (gray). Top chart is a representative example of the staining and gating. Summary of all samples is the bottom chart.  $N = 5-7$  biological replicates; age range of donors is 6 to 69 years. **c** Flow cytometry on PBMC samples to measure intracellular levels of pre-formed cytotoxic molecules in MAIT cells (red) or non-MAIT CD8<sup>+</sup> T cells (gray). Top chart is a representative example of the staining and gating. Summary of all samples is the bottom chart.  $n = 5-10$  biological replicates. **d** T cell clones derived from PBMC or lung BAL fluid were rested or stimulated with T-cell activation beads (anti-CD3/28) overnight and then the collected supernatant was tested by ELISA for the presence of IL-26 cytokine.  $N = 4, 6, 8, 10$  independent clones for blood CD8<sup>+</sup> T cells, blood MAIT cells, lung CD8<sup>+</sup> T cells, and lung MAIT cells. Assay was performed twice with the same results and one of the experiments is displayed. Mean and standard deviation are plotted as error bars. Nonparametric  $T$  tests were used to test differences between groups.

from a panel of both MAIT and non-MAIT T cell clones derived from either the blood or bronchioalveolar lavage (Fig. 4d). TCR stimulation was performed using anti-CD3/28 coated beads. We observed that all of the T cell clones were able to make IL-26 when stimulated through the TCR (Fig. 4d) although MAIT T cell clones derived from the lung made more IL-26 than those derived from the blood. Taken together, MAIT cells in the lung exhibit a polycytotoxic phenotype as a high proportion of them express several granzymes, perforin, granulysin, and can produce IL-26.

**MAIT cells express distinct cytokine receptors including IL-12 and IFN- $\gamma$  receptors.** MR1-independent cytokine-driven responses to bacterial infection have been observed from

circulating and liver-derived MAIT cells. Specifically, these responses have been linked to IL-12 and IL-18. Furthermore, IL-18 and IL-12 p40 are important for the in vivo antibacterial activity of MAIT cells in multiple disease models<sup>1,2,4</sup>. Transcriptome analysis revealed higher gene expression of specific cytokine receptors (Fig. 3a), including *IL23R*, *IFNGR1* (Fig. 5a), and *IL12RB1/2* (Fig. 5b, c) by lung MAIT cells as compared to non-MAIT cells. To assess whether this transcriptional pattern was matched at the protein level, we measured cytokine receptors by flow cytometry on cell populations in blood and lung samples. Here, we observed that a significantly higher proportion of lung and blood MAIT cells expressed IFN- $\gamma$  receptor compared to non-MAIT CD8<sup>+</sup> T cells (Fig. 5a). The IL-12 receptor is comprised of a heterodimer of IL-12 receptor  $\beta 1$  and IL-12 receptor

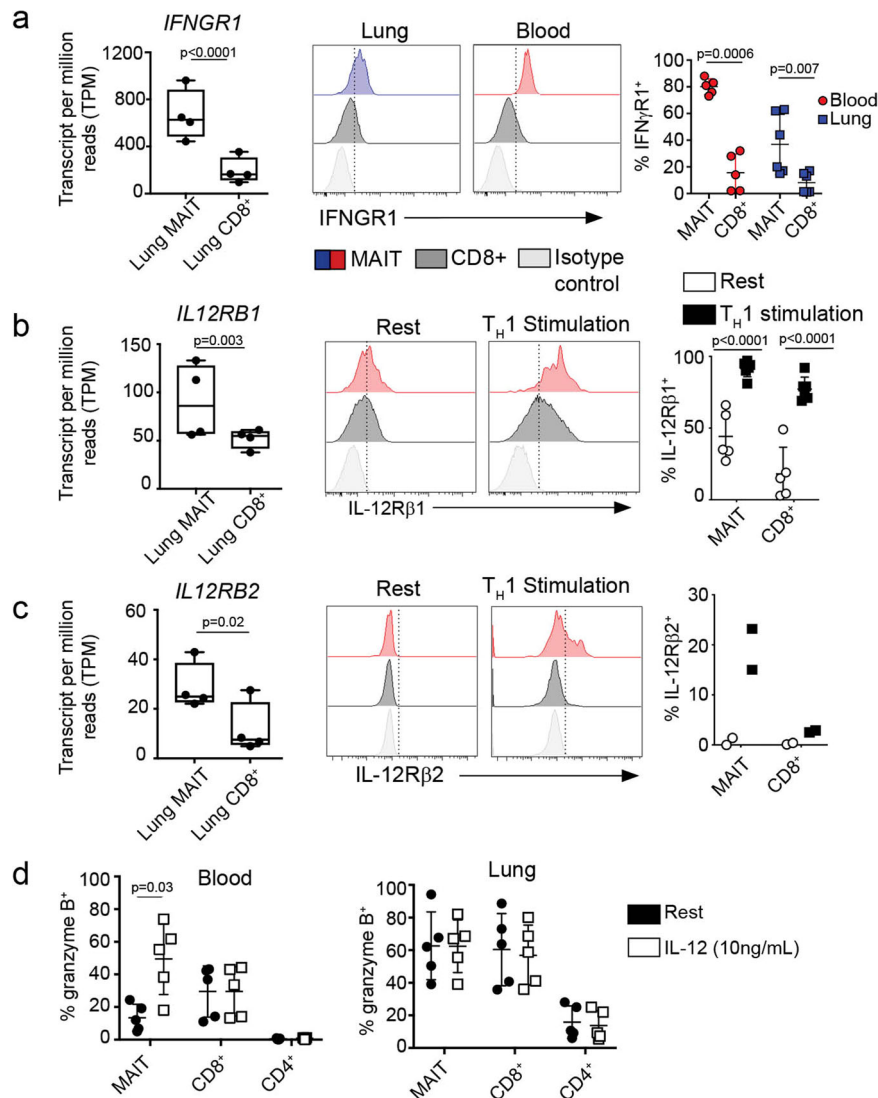


**Fig. 5 IL-12 upregulates granzyme B production in circulating MAIT cells.** **a** Transcripts per million (TPM) of interferon-gamma receptor (*IFNGR1*) in lung MAIT and lung non-MAIT CD8<sup>+</sup> T cells. Ex vivo lung and blood samples were stained with antibody specific for IFN- $\gamma$  receptor on the surface. Histograms show an example of flow cytometry quantification of IFN- $\gamma$  receptor on the gated populations, MR1/5-OP-RU<sup>+</sup> MAIT cells, MR1/5-OP-RU(-) non MAIT CD8<sup>+</sup> T cells, and isotype control staining of CD8<sup>+</sup> T cells. A summary of the frequency of IFNGR1<sup>+</sup> cells is shown on the right,  $n = 5$ . The % of the gated population staining above the isotype control is plotted on the y-axis.; age range of donors is 6 to 69 years. TPM of interleukin 12 receptor B1 (**b**) or B2 (**c**) in lung MAIT, lung non-MAIT CD8<sup>+</sup> T cells samples. Validation at the protein level was performed on PBMC that were rested or stimulated for four days under Th1 conditions including anti-CD3/28, IL-2, and IL12. Lymphocytes were then stained for surface IL-12R  $\beta$ 1 (**b**) or IL-12R $\beta$ 2 (**c**). Staining of MAIT cells (red), non-MAIT CD8<sup>+</sup> T cells (black) or the isotype control (gray) are shown by histograms. Summary of the frequency of IL-12R $\beta$ 1 or  $\beta$ 2 expression of positive cells within that gated population in 5 biological replicates repeated three times. Bar graphs of IL-12R $\beta$ 1 expression represent the mean and SD of the frequency of positive cells within that gated population in 5 biological replicates repeated three times. Bar graphs of IL-12R $\beta$ 2 expression represent the mean and SD of two technical replicates. **d** Cells derived from PBMC or lung samples were either rested (black circles) overnight or in the presence of IL-12 cytokine (white circles, 10 ng/mL) and then stained intracellularly for granzyme B. The frequency of granzyme B positive cells is plotted from 5 PBMC donors (top) and 5 lung donors (bottom). Representative results of three independent experiments are shown,  $n = 5$  biological replicates, age range of donors is 6 to 60 years. Nonparametric *T* tests were used to test differences.

$\beta$ 2. Given that the IL-12 receptor heterodimer is upregulated during inflammation, we measured each receptor separately on resting cells or following four days of stimulation with anti-CD3/28, IL-2, and IL-12. Due to our inability to obtain sufficient lung MAIT cells to culture, these experiments were performed with blood-derived cells. Here, we observed that while a minor fraction of MAIT cells and non-MAIT CD8<sup>+</sup> T cells expressed IL-12RB1 at rest, nearly all of the cells expressed IL-12 receptor B1 following stimulation (Fig. 5b). Additionally, MAIT cells expressed more of the receptor as suggested by comparing the average mean fluorescence intensities of the stimulated populations (CD8<sup>+</sup>: 404

vs. MAIT: 1096). As IL-12 receptor  $\beta$ 1 can pair with IL-23 receptor (for IL-23) or IL-12 receptor  $\beta$ 2 (for IL-12), we also measured IL-23 receptor levels on resting cells and after stimulation. We did not observe IL-23 receptor expression from any of the lung or PBMC samples by flow cytometry using multiple available antibodies. However, when we measured IL-12 receptor  $\beta$ 2 under the same stimulation conditions, we observed that a proportion (on average 19%) of MAIT cells expressed this receptor (Fig. 5c). IL-12 receptor  $\beta$ 2 was not expressed by stimulated non-MAIT CD8<sup>+</sup> T cells.



**MAIT cells respond to IL-12 by upregulating intracellular granzyme B.** Given that few blood-derived MAIT cells expressed granzyme B (Fig. 4c), MAIT cells uniquely expressed IFN- $\gamma$  and IL-12 receptors, and that these cytokines have been implicated in control of intracellular infection, we assessed whether IFN- $\gamma$  and IL-12 could regulate cytotoxic capacity of MAIT cells. To do this, we tested whether IFN- $\gamma$  receptor-, IL-12 receptor-, or TCR-stimulation would regulate the intracellular levels of preformed cytotoxic proteins in MAIT cells or non-MAIT T cells derived from PBMC (Fig. 5d top) and the lung (Fig. 5d bottom). We assessed the frequency of each cell type that expressed granzyme B, granzyme A, granzyme K, perforin, or granulysin by flow cytometry before and after 18-hour stimulation. We observed in blood MAIT cells that only the addition of IL-12 upregulated granzyme B but no other cytotoxic proteins (Fig. 5d, Supplementary Fig. 4). We did not observe changes with IFN- $\gamma$  or TCR stimulation in our *in vitro* assay (Supplementary Fig. 5). The functional signaling consequences of the highly expressed IFN- $\gamma$  receptor on MAIT cells remains to be determined. We note that granzyme B expression is inducible with IL-12 cytokine and thus, IL-12 can license the cytotoxic capacity of circulating MAIT cells which we hypothesize contributes to the higher frequency of granzyme B<sup>+</sup> MAIT cells in the lung.

## Discussion

MAIT cells are an abundant human T cell subset that shares qualities of the innate and adaptive immune system through their recognition of small microbial metabolites presented by MR1. These cells are of particular interest in the setting of respiratory bacterial infection due to their abundance in the airway and demonstrated ability to respond to cells infected with bacteria<sup>20,50,51</sup>. However, an in-depth comparative analysis to reveal fundamental biological pathways of MAIT cells in the human lung has not yet been performed. We undertook a transcriptomic analysis of MAIT cells compared to non-MAIT CD8<sup>+</sup> T cells in the human lung. We found that MAIT cells in the lung display a polycytotoxic phenotype and sense their environment through selective cytokine responsiveness. The lung-derived MAIT cell's gene expression aligns closely with transcriptomics of blood-derived MAIT cells and other innate-like T cell compartments.

Cytokine receptors allow cells to respond to their micro-environment. We found that lung MAIT cells expressed a unique set of cytokine receptors compared to non-MAIT CD8<sup>+</sup> T cells which would contribute to regulating their functions in the lung. The IL-12 receptor and IFN- $\gamma$  receptor were expressed at the protein level by MAIT cells as well. Our staining of IL-12 receptor on MAIT cells supports the recent finding of its expression on MAIT cells derived from lung explants<sup>27</sup>. MAIT cells can become activated by IL-12 and IL-18 in humans, a property thought to be distinctly linked to cell populations expressing *KLRB1/CD161*<sup>52</sup>. A role for IL-12 activation of MAIT cells, independent from MR1, has been described in *in vivo* models of bacterial respiratory infections<sup>2</sup>. As IL-12 is made early in infection by macrophages, DCs, and neutrophils, our data supports the hypothesis that IL-12 receptor expression in MAIT cells facilitates the initial response to infection in the lung.

We observed that lung MAIT cells distinctively expressed transcript for IFN- $\gamma$  receptor compared to non-MAIT CD8<sup>+</sup> T cells. IFN- $\gamma$  cytokine is made upon activation of subsets of NK and T cells and is a critical cytokine in defense against intracellular microbial infection<sup>53</sup>. Given the known roles of signaling through this cytokine, IFN- $\gamma$  receptor activity in MAIT cells likely helps in their polarization towards a Th1 and/or Th17 phenotype and helps them to amplify local cellular immune activation<sup>54</sup>. We also note the expression of the transcription factor *RORC*, known

to be associated with the expression of the cytokine IL-17<sup>55</sup>. While we did observe the expression of *IL17A*, we have not observed protein expression in either peripheral blood MAITs<sup>34</sup> or those in the lung<sup>14</sup>. Interestingly, Cole et al<sup>56</sup> have recently found that MAIT cells express IL-17F rather than IL-17A. However, we did not find expression of IL-17F.

T cells can directly mediate antimicrobial responses through the release of antimicrobial proteins. Here, we confirmed the expression in MAITs of *GZMK*, *PRF* and *GZLY*, characteristic of NK cells and CD8<sup>+</sup> polycytotoxic T lymphocytes<sup>39</sup> and *IL26*, characteristic of Th17 cells<sup>46</sup>, regardless of tissue distribution, which we confirmed by either flow cytometry or ELISA. An analysis of immune-related genes expressed in T cells from human intestinal biopsies also linked *GZMK* to MAIT cells<sup>22</sup>. Together, granzyme B, perforin and granulysin act synergistically to kill intracellular bacteria<sup>38,43,57</sup>. Perforin disrupts the target eukaryotic cell membrane, allowing other cytotoxic proteins to gain access to the inside of the cell. Granzymes are proteases with many host and microbial molecular targets. For example, granzymes can activate host caspases, deactivate host oxidative stress defense proteins, or deactivate bacterial metabolic pathways<sup>57,58</sup>. Furthermore, each granzyme has different proteolytic targets. As MAIT cells expressed high levels of granzyme B, A, and K, this suggests a broad proteolytic spectrum. Granulysin can bind to bacteria damaging its membrane or cell wall<sup>38</sup>. Unexpectedly, the gene encoding the antimicrobial protein, IL-26, was significantly upregulated in MAIT cells. Notably, both MAIT cell clones and non-MAIT cell clones derived from the lung produced IL-26 which required TCR- stimulation. This discrepancy from the core RNA signature pattern could be explained if MAIT cells in the lung are licensed to make IL-26. IL-26 kills extracellular bacteria<sup>46</sup> but can enter macrophages and exert an antimicrobial activity against intracellular bacteria<sup>59</sup>. This suggests that MAIT cells are armed to have broad antimicrobial effector function.

We hypothesized that this polycytotoxic activity could be enhanced as a result of their unique cytokine receptors. In contrast to blood MAIT cells, which express little granzyme B, we found that lung MAIT cells contain preformed granzyme B. Furthermore, we found that *in vitro* stimulation of circulating MAIT cells, but not non-MAIT CD8<sup>+</sup> T cells, with IL-12, but not IFN- $\gamma$ , upregulated intracellular levels of granzyme B. This result would suggest that a cytokine rich lung environment could “license” or augment the cytolytic activity of MAIT cells.

We acknowledge that our bulk RNA-sequencing method may have overlooked functionally distinct MAIT cell subsets. Our transcriptomic analysis was performed directly *ex vivo* so that we could examine their natural state in the lung. Moreover, we had hypothesized that the higher proportion of CD8<sup>-</sup>CD4<sup>-</sup> MAIT cells in the lung may represent a distinct subset at the transcriptomic level and we therefore, performed RNA-seq analysis on these cells separately. Instead, we found very few significant differences in genes upregulated in CD8<sup>-</sup>CD4<sup>-</sup> MAIT cells compared to CD8<sup>+</sup> lung derived MAIT cells. Whether this reflects a common lung environment, or a common lung MAIT precursor the result of imprinting early in life from the microbiome<sup>6</sup>, remains to be determined.

Given MAIT cells' positioning near the epithelium<sup>14</sup>, our findings raise the intriguing possibility that lung-resident MAIT cells could play a specialized role as environmental sensors and immediate effectors upon infection in the airway. Specifically, this could be the result of the release of pro-inflammatory cytokines and chemokines, which assist in the conditioning and migration of myeloid subsets<sup>60</sup>, as well as by their direct anti-microbial activity. MAIT cells are also in a position to directly kill microbes through polycytotoxic mechanisms, a function which is regulated through antigen

specific and innate activation. In the future, how these immune defense pathways change when they become fully activated during a microbial encounter will need to be studied in parallel. Whether these immune defense pathways at the mucosa are successful upon encounter or not could reveal key correlates of a specific immune response.

Finally, the gene profile we have observed would also suggest that MAITs in the lung are poised to tolerate a relatively harsh environment of the airway (*SLC4A10*, *CA2*, and *Aquaporin 3*), or possibly to participate in tissue repair as has been reported by Constantinides et al., and Leng et al.<sup>6,49</sup>. Of relevance to human MAIT cells, Leng et al., found that following MAIT cell stimulation, preferential expression of *Furin* and *CCL3*. They then demonstrated that these genes were associated with tissue repair. While we did not observe preferential expression of these genes, we note that our cells were not specifically stimulated such that we may have missed this phenotype.

## Materials and methods

**Human subjects.** All samples were collected and all experiments were conducted under protocols approved by the institutional review board at Oregon Health and Science University. PBMCs were obtained by apheresis from healthy adult donors with informed consent. De-identified lungs not suitable for transplant were obtained from the Pacific Northwest Transplant Bank (PNTB). Our exclusion criteria included significant tobacco smoking history, drowning, crushing chest injuries, lobar pneumonia, and HIV/HBV/HCV infection. Bronchoalveolar lavage fluid for generating T cell clones was obtained under a protocol approved by the UKZN Biomedical Research Ethics Committee and the Partners Institutional Review Board. The participants provided written informed consent.

**Human tissue sources of T cell populations.** PBMCs were isolated from the peripheral blood of healthy donors using Ficoll-Paque gradients. Lung single cell suspensions are prepared from recently deceased donor tissue not suitable for transplant from the Pacific Northwest Transplant bank. Small cubes of lung parenchyma, devoid of airway and lymph nodes, were cut into a cold buffer of HBSS (Gibco) media supplemented with HEPES (Gibco) and PSF antibiotic (Sigma). Tissue was then digested for 30 min at 37 degrees C in a DMEM buffer (Gibco) supplemented with PSF antibiotics (Sigma), elastase (15 µg/mL, Worthington), trypsin I (1.5 µg/mL, Sigma), DNase I (45 µg/mL, Roche). The subsequent suspension was further dissociated using a GentleMACS dissociator (Miltenyi) using the Lung02 program. The single cell suspension is then diluted 1:1 with a buffer of HBSS (Gibco) media supplemented with 2% heat-inactivated fetal bovine serum (Gemini Bio Products), HEPES (Gibco) and PSF antibiotic (Sigma) to dilute homogenate and neutralize digest enzymes. This cell suspension is passed through successive filters in this order: metal mesh sieve filter (size 40 then 60, Sigma), and nylon cell strainer (100 µm then 40 µm, BD Falcon). The resulting cell suspension is washed in RPMI supplemented with 10% heat inactivated pooled human serum and used for experiments or cryo-preserved in heat-inactivated fetal bovine serum with 10% DMSO. Lung-derived T cell clones were isolated from bronchial alveolar lavage (BAL) samples using a protocol described in detail below.

**Flow cytometry.** All antibodies used in this study are described in Table 1. Cells to be analyzed for cell surface marker expression were blocked with tetramer staining buffer (PBS buffer containing 2% fetal bovine serum). PBMCs were stained with the MR1/5-OP-RU tetramer (NIH Tetramer core facility) at 0.3 nM in 25 µL volume for 45 min in tetramer staining buffer at room temperature in the dark. Viability and surface stains were added on top of the tetramer stain for another 20 min at 4 °C in the dark. Samples were then washed in tetramer staining buffer. For intracellular staining, cells were permeabilized and fixed using the CytoFix/CytoPerm kit (BD) as directed. Antibodies to intracellular proteins were added to samples for 20 min at 4 °C in the dark and then washed with PermWash (BD). Flow cytometry analysis was performed using a LSRFortessa flow cytometer (BD) or a CytoFLEX S flow cytometer (Beckman Coulter). Data were analyzed using FlowJo (v10.4.2). MR1/6-FP tetramer controls were used for optimal gating of MAIT cells. Doublets were excluded based on FSC-H vs. FSC-A and SSC-H vs. SSC-A; T lymphocytes were identified based on FSC-A and SSC-A and CD3 expression; dead cells were excluded based on Aqua viability dye.

**Cell sorting of T cell populations and RNA isolation from sorted cells.** Cells were surface stained using the flow cytometry staining protocol above. Specifically, cells were stained with propidium iodide viability stain, MR1/5-OP-RU tetramer, and antibodies to CD45, CD4, CD8. Lung samples were also stained with antibodies to CD20, CD14, and EpCAM for removal of B cells, myeloid cells, and epithelial cells. Live, CD45<sup>+</sup>, CD4<sup>-</sup>, CD14/CD20/EpCAM<sup>-</sup> were sorted into four populations: MR1/5-OP-RU + CD8<sup>+</sup>, MR1/5-OP-RU + CD8<sup>-</sup>,

negative, MR1/5-OP-RU-negative CD8<sup>+</sup>, and MR1/5-OP-RU-negative CD8<sup>-</sup>. Cells were sorted into TRIzol (Thermo-Fisher) and RNA was isolated using a Direct-zol RNA-mini kit with RNA clean and concentrator columns (Zymo Research) and treated with DNase (Qiagen).

**Quantitative PCR.** Lung cells were sorted directly into 500 µL of RLT buffer in 1.5 mL Eppendorf tubes. 5-OPRU tetramer negative cells were collected as 10,000 cells each and 5-OPRU tetramer positive cells from three lung donors were collected as 3489 cells, 3959 cells and 4730 cells, respectively. Total RNA was isolated using RNeasy mini kit (Qiagen) and eluted with 30 µL of nuclease free water. 9 µL of total RNA samples were proceeded to cDNA synthesis using High Capacity cDNA Reverse Transcription kit (Applied Biosystems). Then, cDNA was amplified using TaqMan PreAmp Master Mix (Applied Biosystems) with assay mix contains GAPDH (Hs02758991\_g1), CD3 (Hs01062241\_m1), CXCR6 (Hs00174843\_m1) and IL-26 (Hs00218189\_m1). The preamplification reaction was done with 14 cycles and reactions were diluted 20 times with TE buffer. The PCR reaction was prepared according to procedure of PreAmp mix and performed with StepOnePlus Real-Time PCR System (Applied Biosystems).

**RNA-sequencing sample preparation.** Sequencing libraries were constructed from total RNA using NuGEN Ovation Ultralow library kit and NuGEN Ovation RNA-seq v2 kit (NuGEN). Libraries were sequenced at OHSU Massively Parallel Sequencing Shared Resource with the Illumina HiSeq platform with single end reads and 100 base read length. An average of 65 million reads were generated for each sample. Data is deposited in NCBI SRA (BioProject ID: PRJNA830885).

**RNAseq transcriptome analysis.** FastQC (<https://www.bioinformatics.babraham.ac.uk/projects/fastqc/>) was used to assess the quality of the raw sequence reads. Reads were then aligned to the Human genome (Hg19) using STAR (version 2.5.2b) (PMID: 23104886) allowing for a maximum of 2 mismatches per 100 bp read. Approximately 85% of reads mapped uniquely to the genome. Read counts per gene were then obtained using HTSeq (PMID: 25260700). Differential gene expression analysis was performed using DESeq2 (PMID: 25516281).

**Generation and characterization of lung derived T cell clones.** Cells from BAL samples were stained with Aqua LIVE/DEAD (Invitrogen), MR1/5-OP-RU tetramer (0.3 nM), α-CD4-FITC (clone OKT4; BioLegend), and α-CD8-APC-Cy7 (clone SK8; BioLegend). Live tetramer-binding cells were sorted the basis of co-receptor expression using an Influx flow cytometer (BD Biosciences), rested overnight in RPMI 1640 supplemented with 10% heat-inactivated pooled human serum and 0.5 ng/ml rIL-2, and distributed in limiting dilution format with irradiated PBMCs and irradiated B-lymphoblastoid cells in a 96-well round bottom plate. The cultures were supplemented with rIL-2 (5 ng/ml), rIL-12 (0.5 ng/ml), rIL-7 (0.5 ng/ml), rIL-15 (0.5 ng/ml) and α-CD3 (0.03 µg/ml). T cell clones were harvested after incubation for 20 days at 37 °C.

**Expansion of T cell clones.** T cell clones were cultured in the presence of x-rayed (3000 cGray using X-RAD320, Precision X-Ray Inc.) allogeneic PBMCs, x-rayed allogeneic LCL (6000 cGray), and anti-CD3 mAb (20 ng/ml; Orthoclone OKT3, eBioscience) in RPMI 1640 media with 10% human serum in a T-25 upright flask in a total volume of 30 ml. The cultures were supplemented with IL-2 on days 1, 4, 7, and 10 of culture. The cell cultures were washed on day 5 to remove soluble anti-CD3 mAb.

**ELISA.** T cell clones were rested for 24 h in RPMI buffer containing 10% human serum and 0.5 ng/mL IL-2. Stimulated cells were mixed 1:2 with MACS Miltenyi Biotec T cell Activation beads. T cell clones were then incubated for 24 h at 37 °C. Cells supernatants were collected and stored at -80 °C. Cytokine secretion was quantified with an IL-26 ELISA kit (Cusabio) according to the manufacturer's instructions.

**T cell in vitro stimulation assays.** To measure IL-12 receptor surface expression, PBMC derived T cells were stimulated for five days at 37 °C with 1 µg/mL anti-CD3 and anti-CD28 and 10 ng/mL of recombinant human IL-2 and recombinant human IL-12p70 (BioLegend). On day four of stimulation, cells were washed with RPMI medium with 10% human serum and 0.5 ng/mL of IL-2 before continuing incubation at 37 °C. Following this five-day period, cells were stimulated with 50 ng/mL of PMA and 200 ng/mL of ionomycin for three hours.

**Statistics and reproducibility.** Statistical analyses were performed using GraphPad Prism 7 software (GraphPad Software Inc., San Diego, CA). Datasets were analyzed for normality using Prism. If normal, a Student's two-tailed *T* test was used for comparisons in Prism. If the data were not normally distributed, the non-parametric *T*-test was used to assess significant differences between groups in Prism. Error bars in the figures indicate the standard deviation, standard error of the mean, or the data set range as indicated in each figure legend. *P* values ≤ 0.05 were considered significant (\**P* ≤ 0.05; \*\**P* ≤ 0.01; \*\*\**P* ≤ 0.001; \*\*\*\**P* ≤ 0.0001).

**Table 1 Antibodies used in this study.**

Target of Antibody	Fluorophore	Manufacturer	Clone	Dilution
CD3	PerCP Cy5.5	BioLegend	SK7	1:50
CD3	PerCP	BD Biosciences	SK7	1:20
CD3	FITC	BioLegend	UCHT1	1:50
CD3	BV421	BioLegend	UCHT1	1:100
CD4	BV785	BioLegend	OKT4	1:200
CD4	FITC	BioLegend	OKT4	1:100
CD8	APC eFluor780	eBioscience	SK1	1:1000
CD8	APC	BioLegend	HITBa	1:100
CD8	FITC	BD Biosciences	RPA-T8	1:100
CD45	BV421	BioLegend	2D1	1:25
CD14	APC	BioLegend	HCD14	1:100
CD20	APC	BioLegend	2H7	1:100
EpCam	APC	BioLegend	9C4	1:25
TRAV1-2	APC	Lewinsohn Lab	OF5A12	1:33
TCR $\alpha\beta$	PE	BD Biosciences	T10B9.1A- 31	1:8
IL-12RB1	PE	BD Biosciences	2.4E6	1:20
Mouse IgG1 Isotype	PE	BioLegend	MOPC-21	a
IL-12RB2	APC	R&D Systems	305719	1:5
Mouse IgG1 Isotype	APC	BD Biosciences	MOPC-21	a
IFNGR1	FITC	R&D Systems	92101	1:10
Mouse IgG1 Isotype	FITC	BioLegend	MOPC-21	a
IL-23R	FITC	R&D Systems	218213	1:10
Mouse IgG2b	FITC	BioLegend	MPC-11	a
Granzyme A	Pac Blue	BioLegend	CB9	1:100
Granzyme B	Pac Blue	BioLegend	QA16A02	1:20
Granzyme K	APC	BioLegend	GM26E7	1:10
Perforin	PE-Cy7	eBioscience (Thermofisher)	dG9	1:200
Granulysin	Alexa Fluor 488	BioLegend	DH2	1:10
CCR7	PE-Cy7	BioLegend	G043H7	1:100
Ms IgG2a Isotype	PE-Cy7	BioLegend	MOPC-173	a
CD62L	PerCP-Cy5.5	BioLegend	DREG-56	1:100
Ms IgG1 Isotype	PerCP-Cy5.5	BioLegend	MOPC-21	a
CD45RO	BV421	BioLegend	UCHL1	1:100
Ms IgG2a Isotype	BV421	BioLegend	MOPC-173	a
CD45RA	FITC	BioLegend	HI100	1:100
Ms IgG2b Isotype	FITC	BioLegend	MPC-11	a
Mouse IgG1 Isotype	Pac Blue	BioLegend	MOPC-21	a
Mouse IgG2b	PE-Cy7	BioLegend	MPC-11	a

<sup>a</sup>isotype concentration matched that used for the corresponding antibodies within experiment.

We determined sample size for our lung cell RNA-sequencing based on power calculations using preexisting similar comparisons of the same analyses on blood-derived MAIT cells.

**Reporting summary.** Further information on research design is available in the Nature Research Reporting Summary linked to this article.

### Data availability

All relevant data are available in this manuscript and from the corresponding author on reasonable request. RNA-seq data is deposited in NCBI SRA (BioProject ID: PRJNA830885). The source data for the figures are contained in Supplementary Data 1.

Received: 19 July 2021; Accepted: 9 August 2022;

Published online: 09 September 2022

### References

- Chua, W. J. et al. Polyclonal MAIT Cells Have Unique Innate Functions in Bacterial Infection. *Infect. Immun.* **80**, 3256–3267 (2012).
- Meierovics, A., Yankelevich, W. J. & Cowley, S. C. MAIT cells are critical for optimal mucosal immune responses during in vivo pulmonary bacterial infection. *Proc. Natl Acad. Sci. USA* **110**, E3119–E3128 (2013).
- Chen, Z. et al. Mucosal-associated invariant T-cell activation and accumulation after in vivo infection depends on microbial riboflavin synthesis and co-stimulatory signals. *Mucosal Immunol.* **10**, 58–68 (2017).
- Wilgenburg, B. V. et al. MAIT cells contribute to protection against lethal influenza infection in vivo. *Nat. Commun.* **9**, 4706 (2018).
- Wang, H. et al. MAIT cells protect against pulmonary *Legionella longbeachae* infection. *Nat. Commun.* **9**, 3350 (2018).
- Constantinides, M. G. et al. MAIT cells are imprinted by the microbiota in early life and promote tissue repair. *Science* **366**, eaax6624 (2019).
- Legoux, F. et al. Microbial metabolites control the thymic development of mucosal-associated invariant T cells. *Science* **366**, 494–499 (2019).
- Gold, M. C. et al. Human thymic MR1-restricted MAIT cells are innate pathogen-reactive effectors that adapt following thymic egress. *Mucosal Immunol.* **6**, 35–44 (2013).
- Swarbrick, G. M. et al. Postnatal Expansion, Maturation, and Functionality of MR1T Cells in Humans. *Front Immunol.* **11**, 556695 (2020).
- Howson, L. J. et al. Absence of mucosal-associated invariant T cells in a person with a homozygous point mutation in MR1. *Sci. Immunol.* **5**, eabc9492 (2020).
- Porcelli, S., Yockey, C. E., Brenner, M. B. & Balk, S. P. Analysis of T cell antigen receptor (TCR) expression by human peripheral blood CD4-8- alpha/beta T cells demonstrates preferential use of several V beta genes and an invariant TCR alpha chain. *J. Exp. Med.* **178**, 1–16 (1993).
- Leeansyah, E., Loh, L., Nixon, D. F. & Sandberg, J. K. Acquisition of innate-like microbial reactivity in mucosal tissues during human fetal MAIT-cell development. *Nat. Commun.* **5**, 3143 (2014).
- Salou, M. et al. A common transcriptomic program acquired in the thymus defines tissue residency of MAIT and NKT subsets. *J. Exp. Med.* **216**, 133–151 (2019).



14. Wong, E. B. et al. TRAV1-2(+) CD8(+) T-cells including oligoclonal expansions of MAIT cells are enriched in the airways in human tuberculosis. *Commun. Biol.* **2**, 203 (2019).
15. Khuzwayo, S. et al. MRI-Restricted MAIT Cells From The Human Lung Mucosal Surface Have Distinct Phenotypic, Functional, and Transcriptomic Features That Are Preserved in HIV Infection. *Front. Immunol.* **12**, 631410 (2021).
16. Yu, H. et al. CXCL16 Stimulates Antigen-Induced MAIT Cell Accumulation but Trafficking During Lung Infection Is CXCR6-Independent. *Front. Immunol.* **11**, 1773 (2020).
17. Shaler, C. R. et al. MAIT cells launch a rapid, robust and distinct hyperinflammatory response to bacterial superantigens and quickly acquire an anergic phenotype that impedes their cognate antimicrobial function: Defining a novel mechanism of superantigen-induced immunopathology and immunosuppression. *PLoS Biol.* **15**, e2001930 (2017).
18. Dusseaux, M. et al. Human MAIT cells are xenobiotic-resistant, tissue-targeted, CD161hi IL-17-secreting T cells. *Blood* **117**, 1250–1259 (2011).
19. Dias, J., Leeanayah, E. & Sandberg, J. K. Multiple layers of heterogeneity and subset diversity in human MAIT cell responses to distinct microorganisms and to innate cytokines. *Proc. Natl Acad. Sci. USA* **114**, E5434–E5443 (2017).
20. Greene, J. M. et al. MRI-restricted mucosal-associated invariant T (MAIT) cells respond to mycobacterial vaccination and infection in nonhuman primates. *Mucosal Immunol.* **10**, 802–813 (2017).
21. Gibbs, A. et al. MAIT cells reside in the female genital mucosa and are biased towards IL-17 and IL-22 production in response to bacterial stimulation. *Mucosal Immunol.* **10**, 35–45 (2017).
22. Slichter, C. K. et al. Distinct activation thresholds of human conventional and innate-like memory T cells. *JCI Insight* **1**, e86292 (2016).
23. Kurioka, A. et al. MAIT cells are licensed through granzyme exchange to kill bacterially sensitized targets. *Mucosal Immunol.* **8**, 429–440 (2015).
24. Le Bourhis, L. et al. MAIT cells detect and efficiently lyse bacterially-infected epithelial cells. *PLoS Pathog.* **9**, e1003681 (2013).
25. Fergusson, J. R. et al. CD161 defines a transcriptional and functional phenotype across distinct human T cell lineages. *Cell Rep.* **9**, 1075–1088 (2014).
26. Leeanayah, E. et al. Arming of MAIT Cell Cytolytic Antimicrobial Activity Is Induced by IL-7 and Defective in HIV-1 Infection. *PLoS Pathog.* **11**, e1005072 (2015).
27. Wallington, J. C., Williams, A. P., Staples, K. J. & Wilkinson, T. M. A. IL-12 and IL-7 synergize to control mucosal-associated invariant T-cell cytotoxic responses to bacterial infection. *J. Allergy Clin. Immunol.* **141**, 2182–2195 e2186 (2018).
28. Kumar, B. V. et al. Human Tissue-Resident Memory T Cells Are Defined by Core Transcriptional and Functional Signatures in Lymphoid and Mucosal Sites. *Cell Rep.* **20**, 2921–2934 (2017).
29. Hombrink, P. et al. Programs for the persistence, vigilance and control of human CD8(+) lung-resident memory T cells. *Nat. Immunol.* **17**, 1467–1478 (2016).
30. Pomazny, M. et al. Quantitative and Qualitative Perturbations of CD8(+) MAITs in Healthy Mycobacterium tuberculosis-Infected Individuals. *Immunohorizons* **4**, 292–307 (2020).
31. Hinks, T. S. C. et al. Activation and In Vivo Evolution of the MAIT Cell Transcriptome in Mice and Humans Reveals Tissue Repair Functionality. *Cell Rep.* **28**, 3249–3262 e3245 (2019).
32. Dias, J. et al. The CD4(-)CD8(-) MAIT cell subpopulation is a functionally distinct subset developmentally related to the main CD8(+) MAIT cell pool. *Proc. Natl Acad. Sci. USA* **115**, E11513–E11522 (2018).
33. Huang, H. et al. Select sequencing of clonally expanded CD8(+) T cells reveals limits to clonal expansion. *Proc. Natl Acad. Sci. USA* **116**, 8995–9001 (2019).
34. Sharma, P. K. et al. High expression of CD26 accurately identifies human bacteria-reactive MRI-restricted MAIT cells. *Immunology* **145**, 443–453 (2015).
35. Olesin, E., Nayar, R., Saikumar-Lakshmi, P. & Berg, L. J. The Transcription Factor Runx2 Is Required for Long-Term Persistence of Antiviral CD8(+) Memory T Cells. *Immunohorizons* **2**, 251–261 (2018).
36. Liu, Y. et al. ADAM12 is a costimulatory molecule that determines Th1 cell fate and mediates tissue inflammation. *Cell Mol. Immunol.* **18**, 1904–1919 (2021).
37. Lee, C. H. et al. C/EBP $\delta$  drives interactions between human MAIT cells and endothelial cells that are important for extravasation. *Elife* **7**, e32532 (2018).
38. Stenger, S. et al. An antimicrobial activity of cytolytic T cells mediated by granulysin. *Science* **282**, 121–125 (1998).
39. Balin, S. J. et al. Human antimicrobial cytotoxic T lymphocytes, defined by NK receptors and antimicrobial proteins, kill intracellular bacteria. *Sci. Immunol.* **3**, eaat7668 (2018).
40. Zhang, N. & Bevan, M. J. CD8(+) T cells: foot soldiers of the immune system. *Immunity* **35**, 161–168 (2011).
41. Lefrancois, L. & Obar, J. J. Once a killer, always a killer: from cytotoxic T cell to memory cell. *Immunol. Rev.* **235**, 206–218 (2010).
42. Bulitta, B. et al. Proteomic definition of human mucosal-associated invariant T cells determines their unique molecular effector phenotype. *Eur. J. Immunol.* **48**, 1336–1349 (2018).
43. Busch, M. et al. Lipoarabinomannan-Responsive Polycytotoxic T Cells Are Associated with Protection in Human Tuberculosis. *Am. J. Respir. Crit. Care Med.* **194**, 345–355 (2016).
44. Sheikh, F. et al. Cutting edge: IL-26 signals through a novel receptor complex composed of IL-20 receptor 1 and IL-10 receptor 2. *J. Immunol.* **172**, 2006–2010 (2004).
45. Stephen-Victor, E., Fickenscher, H. & Bayry, J. IL-26: An Emerging Proinflammatory Member of the IL-10 Cytokine Family with Multifaceted Actions in Antiviral, Antimicrobial, and Autoimmune Responses. *PLoS Pathog.* **12**, e1005624 (2016).
46. Meller, S. et al. T(H)17 cells promote microbial killing and innate immune sensing of DNA via interleukin 26. *Nat. Immunol.* **16**, 970–979 (2015).
47. Dang, A. T. et al. IL-26 contributes to host defense against intracellular bacteria. *J. Clin. Invest.* **130**, 1926–1939 (2019).
48. Lamichhane, R. et al. TCR- or Cytokine-Activated CD8(+) Mucosal-Associated Invariant T Cells Are Rapid Polyfunctional Effectors That Can Coordinate Immune Responses. *Cell Rep.* **28**, 3061–3076 e3065 (2019).
49. Leng, T. et al. TCR and Inflammatory Signals Tune Human MAIT Cells to Exert Specific Tissue Repair and Effector Functions. *Cell Rep.* **28**, 3077–3091 e3075 (2019).
50. Gold, M. C. et al. Human Mucosal Associated Invariant T Cells Detect Bacterially Infected Cells. *PLoS Biol.* **8**, e1000407 (2010).
51. Le Bourhis, L. et al. Antimicrobial activity of mucosal-associated invariant T cells. *Nat. Immunol.* **11**, 701–708 (2010).
52. Ussher, J. E. et al. CD161<sup>++</sup> CD8<sup>+</sup> T cells, including the MAIT cell subset, are specifically activated by IL-12+IL-18 in a TCR-independent manner. *Eur. J. Immunol.* **44**, 195–203 (2014).
53. Boehm, U., Klamp, T., Groot, M. & Howard, J. C. Cellular responses to interferon-gamma. *Annu Rev. Immunol.* **15**, 749–795 (1997).
54. Arlehamn, C. L. et al. Transcriptional profile of tuberculosis antigen-specific T cells reveals novel multifunctional features. *J. Immunol.* **193**, 2931–2940 (2014).
55. De Baldia, M. E. & Bhandoola, A. Transcriptional regulation of innate and adaptive lymphocyte lineages. *Annu Rev. Immunol.* **33**, 607–642 (2015).
56. Cole, S. et al. Interleukin (IL)-12 and IL-18 Synergize to Promote MAIT Cell IL-17A and IL-17F Production Independently of IL-23 Signaling. *Front. Immunol.* **11**, 585134 (2020).
57. Walch, M. et al. Cytotoxic cells kill intracellular bacteria through granulysin-mediated delivery of granzymes. *Cell* **157**, 1309–1323 (2014).
58. Dotiwala, F. et al. Granzyme B Disrupts Central Metabolism and Protein Synthesis in Bacteria to Promote an Immune Cell Death Program. *Cell* **171**, 1125–1137 e1111 (2017).
59. Dang, A. T. et al. IL-26 contributes to host defense against intracellular bacteria. *J. Clin. Invest.* **129**, 1926–1939 (2019).
60. Meierovics, A. I. & Cowley, S. C. MAIT cells promote inflammatory monocyte differentiation into dendritic cells during pulmonary intracellular infection. *J. Exp. Med.* **213**, 2793–2809 (2016).

## Acknowledgements

We thank the Pacific Northwest Transplant Bank for providing tissue samples vital to our investigation. We thank staff of both the OHSU Massively Parallel Sequencing Shared Resource and OHSU Flow Cytometry core. We thank members of the Lewinson lab for technical support and helpful discussions. The following reagents were obtained through the NIH Tetramer Core Facility: MRI/5-OP-RU, MRI/6FP tetramers. The MRI/5-OP-RU tetramer technology was developed jointly by J. McCluskey, J. Rossjohn, and D. Fairlie, and the material was produced by the NIH Tetramer Core Facility as permitted to be distributed by the University of Melbourne. This work was supported by Merit Review Awards I01BX000533 from the United States Department of Veterans Affairs Biomedical Laboratory Research and resources and the use of facilities at the VA Portland Health Care System; NIAID R01AI048090, R01AI134790, U01 AI095776, K08 AI118538; and NHLBI T32HL83808. The contents of this manuscript do not represent the views of the U.S. Department of Veterans Affairs or the United States Government. Research reported in this publication was supported by the Strategic Health Innovation Partnerships (SHIP) Unit of the South African Medical Research Council (SA MRC) with funds received from the South African Department of Science and Technology as part of a bilateral research collaboration agreement with the Government of India; and through a SA MRC Collaborating Centre (ACT4TB/HIV). Additional support was also received through the Sub-Saharan African Network for TB/HIV Research Excellence (SANTHE), a DELTAS Africa Initiative (grant no. DEL-15-006). The DELTAS Africa Initiative is an independent funding scheme of the African Academy of Sciences (AAS)'s Alliance for Accelerating Excellence in Science in Africa (AESA) and supported by the New Partnership for Africa's Development Planning and Coordinating Agency (NEPAD Agency) with funding from the Wellcome Trust 107752/Z/15/Z and the UK government.



### Author contributions

Conception and design—E.W.M., C.L.Z., M.C.G., D.M.L.; Acquisition of data—E.W.M., J.G.T., D.I.W., E.K., S.K., G.S., S.S., A.W.; Analysis and interpretation of data—all authors; Drafting of manuscript—E.W.M., D.M.L.; revisions and approval of manuscript—all authors.

### Competing interests

The authors declare no competing interests.

### Additional information

**Supplementary information** The online version contains supplementary material available at <https://doi.org/10.1038/s42003-022-03823-w>.

**Correspondence** and requests for materials should be addressed to David M. Lewinsohn.

**Peer review information** *Communications Biology* thanks Johan Sandberg and the other, anonymous, reviewer(s) for their contribution to the peer review of this work. Primary Handling Editors: Damon Tumes and Zhijuan Qiu.

**Reprints and permission information** is available at <http://www.nature.com/reprints>

**Publisher's note** Springer Nature remains neutral with regard to jurisdictional claims in published maps and institutional affiliations.



**Open Access** This article is licensed under a Creative Commons Attribution 4.0 International License, which permits use, sharing, adaptation, distribution and reproduction in any medium or format, as long as you give appropriate credit to the original author(s) and the source, provide a link to the Creative Commons license, and indicate if changes were made. The images or other third party material in this article are included in the article's Creative Commons license, unless indicated otherwise in a credit line to the material. If material is not included in the article's Creative Commons license and your intended use is not permitted by statutory regulation or exceeds the permitted use, you will need to obtain permission directly from the copyright holder. To view a copy of this license, visit <http://creativecommons.org/licenses/by/4.0/>.

This is a U.S. Government work and not under copyright protection in the US; foreign copyright protection may apply 2022